Journal Pre-proof

Loss of apolipoprotein E contributes to inflammatory macrophage activation and ferroptosis in NSAID-exacerbated respiratory disease

Gilles Schmiz, Pascal Haimerl, PhD, Isika Ram, MSc, Manuel Kulagin, Benedikt Spitzlberger, MSc, Fiona D.R. Henkel, PhD, Franziska Hartung, PhD, Sonja Schindela, Zhigang Rao, PhD, Andreas Koeberle, PhD, Carsten B. Schmidt-Weber, PhD, Adam M. Chaker, MD, Antonie Lechner, PhD, , Julia Esser-von Bieren, PhD

PII: S0091-6749(25)00652-9

DOI: https://doi.org/10.1016/j.jaci.2025.06.010

Reference: YMAI 16832

To appear in: *Journal of Allergy and Clinical Immunology*

Received Date: 5 August 2024

Revised Date: 21 May 2025

Accepted Date: 6 June 2025

Please cite this article as: Schmiz G, Haimerl P, Ram I, Kulagin M, Spitzlberger B, Henkel FDR, Hartung F, Schindela S, Rao Z, Koeberle A, Schmidt-Weber CB, Chaker AM, Lechner A, Bieren JE-v, Loss of apolipoprotein E contributes to inflammatory macrophage activation and ferroptosis in NSAID-exacerbated respiratory disease, *Journal of Allergy and Clinical Immunology* (2025), doi: https://doi.org/10.1016/j.jaci.2025.06.010.

Loss of apolipoprotein E contributes to inflammatory macrophage activation and ferroptosis in NSAID-exacerbated respiratory disease

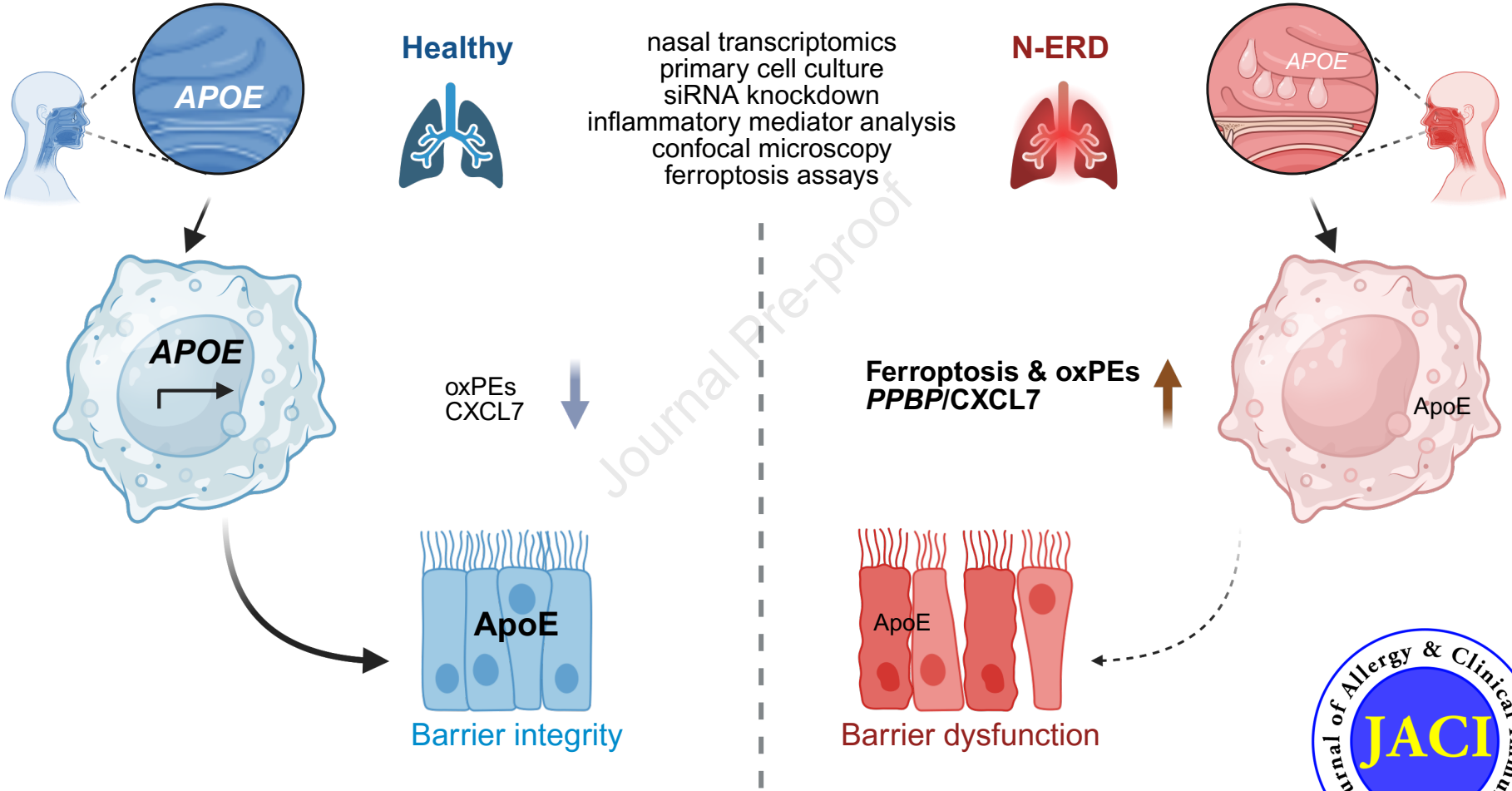

ApoE: apolipoprotein E, oxPE: oxidized arachidonyl phosphatidyl ethanolamines, N-ERD: NSAID-exacerbated respiratory disease, NSAID: non-steroidal anti-inflammatory drugs

Loss of apolipoprotein E contributes to inflammatory macrophage activation and ferroptosis in NSAID-exacerbated respiratory disease

Gilles Schmiz[1], Pascal Haimerl PhD[1], Isika Ram MSc[2], Manuel Kulagin[2], Benedikt Spitzlberger MSc[1], Fiona D.R. Henkel PhD[1], Franziska Hartung PhD[1], Sonja Schindela[1], Zhigang Rao PhD[3], Andreas Koeberle PhD[3,4], Carsten B. Schmidt-Weber PhD[1], Adam M. Chaker MD[1,5], Antonie Lechner PhD[1,6]*, Julia Esser-von Bieren PhD[1,2]*

[1]Center of Allergy and Environment (ZAUM), Technical University of Munich (TUM) and Helmholtz Center Munich, 80802 Munich, Germany

[2]Department of Immunobiology, University of Lausanne, 1066 Epalinges, Switzerland

[3]Michael Popp Institute and Center for Molecular Biosciences Innsbruck (CMBI), University of Innsbruck, 6020 Innsbruck, Austria

[4]Institute of Pharmaceutical Sciences and Excellence Field BioHealth, University of Graz, 8010 Graz, Austria

[5]Department of Otorhinolaryngology and Head and Neck Surgery, TUM School of Medicine and Health, Technical University of Munich, 81675 Munich, Germany

[6]current address: Institute of Physiology, University of Zürich, 8057 Zürich, Switzerland

* shared senior authors

Correspondence:

Julia Esser-von Bieren, Department of Immunobiology, University of Lausanne, 1066 Epalinges, Switzerland Phone: 0041216925723 Fax: 0041216925705 Email: julia.esser-vonbieren@unil.ch

Antonie Lechner, Institute of Physiology, University of Zurich, 8057 Zurich, Switzerland; Phone: 0041440354042 Fax: 0041446356814 Email: toni.lechnerfriedl@uzh.ch

Funding Information

This study was supported by the Else Kröner-Fresenius-Stiftung (grant 2015_A195), the German Research Foundation (DFG) (FOR2599, ES 471/3-2; ES 471/2-3; SPP2306, ES 471/6-1; 490846870–TRR355/1 TPB09), the Fritz Thyssen Stiftung (grant Az. 10.17.2.017MN), the Swiss National Science Foundation grant 310030_212312 and a Helmholtz Young Investigator grant (VH-NG-1331) to J.E.v.B. A.K. was funded by the Phospholipid Research Center (AKO-2022-100/2-2) and the Austrian Science Fund (FWF) (10.55776/P36299), and Z.R. by the Tyrolean Science Fund (TWF) (F.33467/7-2021). A.L. was funded by a Leopoldina Postdoctoral Fellowship (LPDS 2022-07).

Disclosure statement

C. B. Schmidt-Weber received grant support from Allergopharma, PLS Design, as well as Zeller AG; and received speaker honoraria from Allergopharma. AMC reports grants, speaker honoraria, consultancy or advisory fees and/or research support and other, all via Technical University of Munich from Allergopharma, ALK Abello, Astra Zeneca, Bencard/Allergen Therapeutics, GSK, Novartis, Hippo Dx, LETI, Roche, Zeller, Sanofi, Regeneron, Thermo Fisher Scientific, EIT Health and Federal Ministery of Research and Education Germany, all outside this submitted work. The rest of the authors declare that they have no relevant conflicts of interest.

Abstract

Background: NSAID-exacerbated respiratory disease (N-ERD) is characterized by chronic asthma, nasal polyposis and intolerance to nonsteroidal anti-inflammatory drugs. We have recently described aberrant macrophage activation and lipid metabolism in N-ERD, however local drivers of nasal inflammation in N-ERD are incompletely understood.

Objective: To study how apolipoprotein E deficiency in the N-ERD nasal mucosa affects the crosstalk and inflammatory activation of macrophages and epithelial cells. *Methods*: We combined transcriptional and mediator analysis of N-ERD patient samples and primary human cell culture to study ApoE in epithelial and myeloid cells. *Results:* N-ERD nasal scrapings exhibited decreased *APOE* expression in comparison to healthy nasal mucosa, but *APOE* was inherently low in epithelial cells. Instead, myeloid cells expressed highly abundant *APOE*, which was reduced in monocyte-derived macrophages from N-ERD patients. siRNA-mediated knockdown of *APOE* in monocyte-derived macrophages resulted in increased CXCL7 expression, an inflammatory chemokine implicated in N-ERD. In addition, highly oxidized arachidonyl-phosphatidylethanolamine accumulated in *APOE*-knockdown macrophages and ApoE protected macrophages from ferroptotic cell death. *Conclusion*: Our results suggest a role for myeloid ApoE in regulating the crosstalk between macrophages and epithelial cells as well as ferroptosis during type 2 airway inflammation. ApoE deficiency may thus contribute to chronic type 2 inflammation in N-ERD, and its restoration could help reestablish normal epithelial barrier integrity and macrophage effector functions.

Key Messages

- apolipoprotein E is reduced in N-ERD nasal mucosa and macrophages
- macrophages and epithelium may communicate via ApoE
- ApoE regulates CXCL7 and macrophage ferroptosis in type 2 inflammation

Capsule Summary

Downregulation of myeloid apolipoprotein E drives increased macrophage CXCL7 production and lipid peroxidation, thus contributing to inflammation and barrier dysfunction in N-ERD.

Key Words

Macrophage; NSAID-exacerbated respiratory disease; Innate immunity; Mucosal immunology; Apolipoprotein; Ferroptosis

Abbreviations

ApoE	apolipoprotein E
GC	glucocorticoid
kd	knockdown
MDM	monocyte-derived macrophage
NSAID	non-steroidal anti-inflammatory drugs
N-ERD	NSAID-exacerbated respiratory disease
NP	nasal polyposis

PGE_2	prostaglandin E_2
ZO-1	Zonula Occludens protein 1

Main text

Introduction

Intolerance to nonsteroidal anti-inflammatory drugs (NSAID), nasal polyposis (NP) and chronic bronchial asthma are hallmarks of NSAID-exacerbated respiratory disease (N-ERD). N-ERD patients suffer from anosmia and refractory polyposis, which lead to a high nasal symptom burden and decreased quality of life (1). Aberrant eicosanoid lipid mediator signaling plays an important role in N-ERD etiology as PGE_2 signaling and production are impaired while cysteinyl leukotrienes cause eosinophilic nasal and bronchial inflammation (1). In addition, we have recently shown aberrant macrophage activation and lipid metabolism in N-ERD (2). Here, we studied whether lipid metabolism changes in macrophages affect the crosstalk with epithelial cells and consequently nasal inflammation in N-ERD. Using transcriptomic analysis of nasal mucosa samples from N-ERD patients and examining the effects of downregulated APOE in the crosstalk between macrophages and epithelial cells, we identify ApoE deficiency as a driver of inflammation and lipid peroxidation in N-ERD.

Results and discussion

We analyzed the transcriptome of nasal mucosal samples from 4 previously described N-ERD patients and 3 age- and sex-matched healthy individuals (2). For detailed methods, please see the Methods section in this article's Online Repository at www.jacionline.org. Differentially expressed genes were related to lipid metabolism and immune regulation (Fig.1A-C). Apolipoprotein genes *APOE* and *APOC1* were downregulated in N-ERD and lipoprotein metabolism and lipid mobilization pathways were enriched (Fig.1C). Upregulation of the glucocorticoid (GC) receptor response gene *FKBP5* in N-ERD epithelium reflected continuous GC application of N-ERD patients (Fig.1A,B). We confirmed diminished ApoE protein in N-ERD NP tissues

compared to healthy turbinates (Fig.1D,E). ApoE staining was not restricted to a specific epithelial cell subtype such as goblet (Muc5A), basal (p63), ciliated (acetylated tubulin) or club cells (uteroglobin), but was found throughout the epithelium, including in $CD68^+$ macrophages (Fig.1F,G). ApoE staining of macrophages in the turbinate tissue was less bright than expected potentially due to the constitutive secretion of ApoE (3). Indeed, freshly translated ApoE contains a secretory signal peptide, which is lost following uptake (3). This likely explains the discrepancy between intracellular ApoE levels *in situ* (Fig.1G) and ApoE secretion *ex vivo* (Fig.1H). GC or inflammatory stimuli did not affect *APOE* expression in air-liquid-interface cultured normal human bronchial epithelial cells (ALI-NHBE) (Fig.1J-L), excluding GC treatment or epithelial inflammation as drivers of *APOE* downregulation.

Macrophages represent a major source of ApoE which protects against atherosclerosis and airway inflammation (4–6). Macrophages differentiated from healthy human monocytes with M-CSF (MDM) or GM-CSF and TGFβ (aMDM), simulating the airway milieu (7), produced more ApoE than NHBE (Fig.1H,I), suggesting that macrophages represent a major source of ApoE particularly in the lower airways and that lack of ApoE in these cells may contribute to airway inflammation in N-ERD. Indeed, previous transcriptomic analysis had revealed *APOE* downregulation in aMDM of N-ERD patients (2) which we independently confirmed in additionally recruited patients and healthy controls (Fig.2A). Characteristics of these patients are described in Table 1. *APOE* expression was uniformly low in CD14-depleted PBMCs, supporting myeloid cells as a dominant source of *APOE* (Fig.2B). Macrophages found in the nasal tissue (Fig.1G) may thus secrete ApoE into their environment. GC, IL-4, or IL-6 did not suppress *APOE* in aMDM (Fig.2C,D) and prolonged GC exposure (6 days) rather induced macrophage *APOE* expression alongside *FKBP5* (Fig.2E,F). When studying

functional roles of ApoE in epithelium by exogenously adding ApoE, we did not observe effects on pro- or anti-inflammatory gene transcription at baseline or during house dust mite (HDM) stimulation (Fig.2G-J). This contrasts previous studies reporting an ApoE-mediated TLR4-dependent activation of epithelial cells (8), potentially due to the different origin and lower LPS content of ApoE protein used in our study or a different LPS response in epithelial cells from asthmatic patients (8) as compared to NHBE from healthy donors (our study). NHBE internalized ApoE from the medium or from macrophage supernatant (Fig.3A,B), showing that epithelial cells may acquire ApoE from the environment. Epithelial ApoE content increased to a lesser degree if NHBE were exposed to N-ERD aMDM supernatants compared to supernatant of aMDM from healthy donors (Fig.3B,C). In addition, the uptake of exogenous recombinant ApoE could be partially blocked by Receptor-Associated Protein (RAP), an endogenous inhibitor of the low-density lipoprotein receptor-related protein 1 (LRP1) receptor (Fig.3D,E). As macrophage *APOE* expression strongly exceeded epithelial *APOE* (Fig.1I), the reduced *APOE* levels in nasal scrapings may reflect diminished myeloid *APOE* expression of N-ERD patients. Indeed, transcriptomes were acquired from all cells present in the mucosa and as macrophages can express high levels of *APOE* (Fig.1H,I), their presence may disproportionately contribute to overall read counts. A defective crosstalk between macrophages and the airway epithelium due to reduced myeloid ApoE may contribute to barrier impairment and chronic type 2 inflammation in N-ERD. Indeed, NHBE exposed to healthy aMDM supernatant tended to increase the tight junction protein ZO-1 while N-ERD aMDM supernatant did not have this effect (Fig.3B,F). aMDM downregulated *APOE* in response to HDM or lipopolysaccharide (LPS) exposure in a TLR4-dependent fashion (Fig.3G) while other HDM sensors (9,10) did not participate (Fig.3H). This suggests that suppression of airway ApoE may be due to exogenous microbial factors rather than due to inflammatory host factors or GC.

A recent study in mice showed that ApoE regulates the differentiation of MDM in lungs upon β-glucan exposure and that ApoE-dependent MDM enhanced protection against bacterial infection (6). To study functional consequences of reduced macrophage *APOE* expression in the context of N-ERD, we performed siRNA knockdown (kd) of *APOE* in aMDM. (Fig.4A,B). Upon HDM stimulation, *APOE*-kd aMDM produced more *PPBP* (CXCL7), implicated in N-ERD (11) while other cytokines were not affected (Fig.4C,D). Thus, ApoE regulates N-ERD-related mediators rather than generally affecting macrophage activation.

Dysregulated lipid mediator metabolism plays a key role in N-ERD pathology (12). As the synthesis and signaling of the regulatory eicosanoid prostaglandin (PG) E_2 is defective in N-ERD, we studied whether ApoE affects PGE_2 production of macrophages. Exogenous ApoE rather reduced PGE_2 levels (Fig.4E), while *APOE*-kd tended to increase the PGE_2 pathway (Fig.4F,G), suggesting that reduced ApoE is not responsible for the aberrant PGE_2 metabolism in N-ERD.

In addition to the role of *APOE* isoforms in Alzheimer`s disease, ApoE was recently described as an inhibitor of ferroptosis in neurons (13). Ferroptosis is an oxidative cell death associated with type 2 inflammation, and we observed that exogenous ApoE decreased aMDM cell death (Fig.4H), while *APOE*-kd increased highly oxidized arachidonyl-phosphatidylethanolamine (oxPE, C18:0/C20:4), a major ferroptosis-inducing lipid species (14) (Fig.4I). Consistent with ApoE's protective role against lipid peroxidation and ferroptosis in human MDM, bone-marrow-derived macrophages (BMDM) from *Apoe*$^{-/-}$ mice exhibited increased susceptibility to ferroptosis compared to those from wild-type mice, a vulnerability that was mitigated by the addition of exogenous ApoE (Fig.4J). In line with its previously published functions as an antioxidant or metal-binding agent, ApoE may restrict lipid peroxidation and ferroptosis in the airways. In N-ERD, this safeguarding function may be impaired due to a

deficiency of myeloid ApoE. It will be interesting to discern if ApoE deficiency is more broadly involved in aberrant macrophage activation and ferroptosis under type 2 inflammatory conditions such as asthma or rhinitis. While our data does not indicate reduced ApoE levels in nasal polyp tissue from patients with chronic rhinosinusitis with nasal polyposis (CRSwNP) (Fig.1G), additional research is required to determine whether ApoE downregulation is a feature that discriminates N-ERD from CRSwNP. The current study highlights the need for further investigation into ApoE-regulated lipid homeostasis in macrophages, with the goal of improving therapy options for N-ERD and potentially other chronic inflammatory respiratory diseases.

Acknowledgements

The authors thank the study participants, as well as Jana Hartmann, Jana Sänger and Silvia de la Morte for excellent technical support.

References

1. Laidlaw TM, Levy JM. NSAID-ERD Syndrome: the New Hope from Prevention, Early Diagnosis, and New Therapeutic Targets. Curr Allergy Asthma Rep. 2020 Mar 14;20(4):10.
2. Haimerl P, Bernhardt U, Schindela S, Henkel FDR, Lechner A, Zissler UM, et al. Inflammatory macrophage memory in NSAID-exacerbated respiratory disease. J Allergy Clin Immunol. 2020 Jun;S0091674920308034.
3. Zannis VI, McPherson J, Goldberger G, Karathanasis SK, Breslow JL. Synthesis, intracellular processing, and signal peptide of human apolipoprotein E. J Biol Chem. 1984 May 10;259(9):5495–9.
4. Yao X, Fredriksson K, Yu ZX, Xu X, Raghavachari N, Keeran KJ, et al. Apolipoprotein E negatively regulates house dust mite-induced asthma via a low-

density lipoprotein receptor-mediated pathway. Am J Respir Crit Care Med. 2010 Nov 15;182(10):1228–38.

5. Linton MF, Atkinson JB, Fazio S. Prevention of Atherosclerosis in Apolipoprotein E-Deficient Mice by Bone Marrow Transplantation. Science. 1995 Feb 17;267(5200):1034–7.

6. Theobald H, Bejarano DA, Katzmarski N, Haub J, Schulte-Schrepping J, Yu J, et al. Apolipoprotein E controls Dectin-1-dependent development of monocyte-derived alveolar macrophages upon pulmonary β-glucan-induced inflammatory adaptation. Nat Immunol [Internet]. 2024 Apr 26 [cited 2024 May 30]; Available from: https://www.nature.com/articles/s41590-024-01830-z

7. Henkel FDR, Friedl A, Haid M, Thomas D, Bouchery T, Haimerl P, et al. House dust mite drives pro-inflammatory eicosanoid reprogramming and macrophage effector functions. Allergy [Internet]. 2018 Dec 16 [cited 2019 Jan 31]; Available from: https://onlinelibrary.wiley.com/doi/abs/10.1111/all.13700

8. Kalchiem-Dekel O, Yao X, Barochia AV, Kaler M, Figueroa DM, Karkowsky WB, et al. Apolipoprotein E Signals via TLR4 to Induce CXCL5 Secretion by Asthmatic Airway Epithelial Cells. Am J Respir Cell Mol Biol. 2020 Aug;63(2):185–97.

9. Barrett NA, Maekawa A, Rahman OM, Austen KF, Kanaoka Y. Dectin-2 recognition of house dust mite triggers cysteinyl leukotriene generation by dendritic cells. J Immunol Baltim Md 1950. 2009 Jan 15;182(2):1119–28.

10. Lechner A, Henkel F, Hartung F, Bohnacker S, Alessandrini F, Gubernatorova EO, et al. Macrophages acquire a TNF-dependent inflammatory memory in allergic asthma. J Allergy Clin Immunol. 2021 Dec;S009167492102741X.

11. Liu T, Barrett NA, Kanaoka Y, Buchheit K, Laidlaw TM, Garofalo D, et al. Cysteinyl leukotriene receptor 2 drives lung immunopathology through a platelet

and high mobility box 1-dependent mechanism. Mucosal Immunol. 2019;12(3):679–90.

12. Laidlaw TM, Boyce JA. Aspirin-Exacerbated Respiratory Disease—New Prime Suspects. N Engl J Med. 2016;374(5):484–8.

13. Belaidi AA, Masaldan S, Southon A, Kalinowski P, Acevedo K, Appukuttan AT, et al. Apolipoprotein E potently inhibits ferroptosis by blocking ferritinophagy. Mol Psychiatry. 2022 Apr 28;

14. Kagan VE, Mao G, Qu F, Angeli JPF, Doll S, Croix CS, et al. Oxidized arachidonic and adrenic PEs navigate cells to ferroptosis. Nat Chem Biol. 2017 Jan;13(1):81–90.

Table 1: Patient characteristics

	healthy		N-ERD	
Age (SDV)	42	(14)	57	(18)
Sex (F)	4/4		7/7	
Physician-diagnosed asthma	0/4		7/7	
Reports NSAID-triggered bronchial hyperreactivity	0/4		7/7	

Figure Legends

Figure 1: *APOE* is downregulated in nasal tissue of N-ERD patients independently of steroid treatment

A-C: Nasal scraping transcriptomics from N-ERD patients and healthy donors **D-E**: Representative images (D) and quantification (E) of ApoE in turbinates (healthy, n=3) and nasal polyps (N-ERD, n=5), scale bar 50 µm **F**: Representative images of immunohistochemistry staining for ApoE and epithelial cell type markers, scale bar 100 µm **G**: Representative images of immunofluorescence staining for ApoE and CD68 in turbinate of healthy control or nasal polyp tissue of N-ERD or CRSwNP patients, arrows indicate $ApoE^{+}$ $CD68^{+}$ cells, scale bar 20 µm **H-I**: Comparison of *APOE* expression (n=4-9, 1way ANOVA with Tukey's MC test) (H) or ApoE secretion (I) (n=2-6, Kruskal-Wallis test with Dunn's MC test) **J**: Representative images of ApoE localization in ALI-cultured NHBE ± Fluticasone proprionate, scale bar 50 µm **K-L**: *APOE* expression in ALI-NHBE ± inflammatory stimuli (K) or ± fluticasone (L) (n=4, Wilcoxon test) for 24h. *p<.05, **p<0.01, ***p<0.001, ns=not significant, ALI=air-liquid interface.

Figure 2: ApoE is downregulated in myeloid cells from N-ERD patients but unchanged by inflammation in epithelium

A-B: *APOE* expression in aMDM (A) or in CD14⁻ PBMC (B) from healthy donors or N-ERD patients (n=3-9, Mann-Whitney test) **C**: *APOE* expression in aMDM ± fluticasone or IL-4 24h (n=6, Wilcoxon test) **D**: ApoE secretion from aMDM ± pro- or anti-inflammatory stimulation (24h) (n=3, Wilcoxon test) **E-F**: *APOE* (E) or *FKBP5* (F) expression in aMDM after prolonged GC treatment (n=3, Friedmann test with Dunn's MC test) **G-J:** Gene expression in NHBE ± rising concentrations of ApoE (24h, n=4) (G, H) or ± HDM stimulation after 24h ApoE treatment (n=4, 2way ANOVA with Sidak's MC test) * p<0.05, ** p<0.01, ***p<0.001, ns=not significant

Figure 3: Macrophages dynamically regulate *APOE* and secrete it for epithelial uptake

A: Representative images of ApoE content in NHBE exposed to ApoE or aMDM-supernatant, scale bar: 20 µm. **B-C**: Representative images (B) and quantification (C) of ApoE content of NHBE exposed to aMDM supernatant from healthy controls or N-ERD patients (n=3, Kruskal-Wallis test) scale bar 20 µm **D-E**: Quantification (D) and representative images (E) of ApoE content in NHBE exposed to ApoE ± RAP (n=3, Kruskal-Wallis test) **F**: Quantification of ZO-1 in NHBE exposed to aMDM supernatant from healthy controls or N-ERD patients (n=3) **G-H**: ApoE secretion or *APOE* expression in aMDM ± HDM or ± TLR4 block followed by LPS stimulation (0.1 or 1.0 ng/mL) (24h, n=4, Friedmann test with Dunn's MC test) (G), or (H) ± dectin-2 or FPR2 block followed by HDM activation (n=3,1way ANOVA with Holm-Sidak's MC test) *p<.05, **p<0.01, ns=not significant, SN=supernatant

Figure 4: ApoE regulates CXCL7/PPBP and ferroptosis in macrophages

A, B: *APOE* expression (A) or ApoE secretion (B) of aMDM after 48h treatment with scrambled (non-targeting) or *APOE* siRNA (n=8, paired *t* test) **C**: *PPBP* expression after HDM stimulation in scrambled or *APOE* siRNA treated aMDM (n=8, 2way ANOVA with Sidak's MC test) **D**: Fold change HDM versus control of cytokine/chemokine production from aMDM after transduction with scrambled or *APOE*-targeting siRNA ± HDM stimulation (24h, n= 3-8, Kruskal-Wallis test) **E-F**: PGE_2 production after HDM stimulation (24h) in PBS- or ApoE-treated aMDM (E) or scrambled or *APOE*-siRNA treated aMDM (F) (n=4-6, ELISA, 2way ANOVA with Sidak's MC test) **G**: Gene expression of PGE_2-biosynthetic enzymes of aMDM after transduction with scrambled or *APOE*-targeting siRNA ± HDM stimulation (24h, n=8-9, 2way ANOVA with Sidak's MC test) **H**: Suppression of RSL3-induced ferroptotic cell death in aMDM treated with exogenous ApoE **I**: oxidized 1-palmitoyl-2-arachidonoyl-*sn*-glycerol-3-phosphoethanolamine (oxPE) species in scrambled or *APOE* siRNA treated aMDM (n=6, Wilcoxon test) **J**: Cell death as indicated by Sytox Green signal (GCU= green calilbrated unit) in wildtype or *Apoe*$^{-/-}$ BMDM ± 24h RSL3 ± 6.8 µg/mL ApoE (n=3-4, 2way ANOVA) *p<0.05, **p<0.01, ns=not significant, WT = wildtype

Online Repository

Loss of apolipoprotein E contributes to inflammatory macrophage activation and ferroptosis in NSAID-exacerbated respiratory disease

Gilles Schmiz[1], Pascal Haimerl PhD[1], Isika Ram MSc[2], Manuel Kulagin[2], Benedikt Spitzlberger MSc[1], Fiona D.R. Henkel PhD[1], Franziska Hartung PhD[1], Sonja Schindela[1], Zhigang Rao PhD[3], Andreas Koeberle PhD[3,4], Carsten B. Schmidt-Weber PhD[1], Adam M. Chaker MD[1,5], Antonie Lechner PhD[1,6]*, Julia Esser-von Bieren PhD[1,2]*

Detailed methods and materials are provided in this Online Repository and include the following:

- **METHOD DETAILS**
  - **Patients**
  - **Mice**
  - **Cell isolation and culture**
  - **siRNA knockdown**
  - **ELISA**
  - **Immunohistochemistry, immunofluorescence staining and confocal microscopy**
  - **Ferroptosis analysis**
  - **RNA extraction and qPCR**
- **QUANTIFICATION AND STATISTICAL ANALYSIS**
  - **Transcriptomics**
  - **Lipid extraction and targeted redox lipidomics**
  - **Statistical analysis**

- **Extended Tables and Legends**

METHOD DETAILS

Patients

Patients with N-ERD and healthy controls were recruited according to their clinical characteristics at the otorhinolaryngology department of the Klinikum rechts der Isar (Munich, Germany) as previously described (1,2). Healthy controls had no history of chronic rhinosinusitis, nasal polyposis, allergy, asthma, or intolerance to NSAID. N-ERD was defined as physician-diagnosed chronic asthma, CRSwNP, and a history of respiratory reactions to oral NSAID. Participants provided a blood sample for PBMC isolation and curettage sample of turbinate (healthy control) or nasal polyp (N-ERD) mucosa for transcriptome analysis after giving informed written consent in accordance with the Declaration of Helsinki. Nasal polyp tissue from N-ERD patients or turbinates from healthy probands acquired by functional endoscopic sinus surgery were used for immunofluorescence stainings after informed written consent.

Mice

C57BL/6J mice were obtained from Charles River Laboratories (Sulzfeld). *Apoe*$^{-/-}$ mice (B6.129P2-Apoe^{tm1Unc}/J) were a kind gift from Dr. Maxime Pellegrin, Service d'Angiologie, University of Lausanne, Switzerland. Mice were maintained under a 12h/12h light/dark cycle in specific pathogen free conditions at the University of Lausanne with *ad libitum* access to food and water. Unless stated otherwise, 6- to 12-week-old mice of both sexes were used. All animal experiments were approved by the local authorities (Canton de Vaud, VD3809c).

Cell isolation and culture

Monocyte-derived macrophages: CD14^{+} monocytes were separated from PBMC extracted *via* density gradient (Lymphoprep, Abbott Diagnostics Technologies) using magnetic beads (CD14 Micro Beads, Miltenyi, Bergisch-Gladbach, Germany), then differentiated in RPMI-1640 with 10% fetal bovine serum, 2 mmol/L L-glutamine, 100 U/mL penicillin/streptomycin and 10 ng/mL gentamicin (all Thermo Fisher, Waltham, MA, USA) at 37°C and 5% CO_2 for 6 days. aMDM were differentiated in medium supplemented with 10 ng/mL rhGM-CSF (Miltenyi) and 2 ng/mL rhTGFβ1 (PeproTech, Hamburg, Germany) and MDM in medium containing 20 ng/mL rhM-CSF (Miltenyi). Macrophages were replated on day 6 for stimulation with ApoE (8.5-8500 ng/mL, Merck), LPS (0.1-1.0 ng/mL, Invivogen, Toulouse, France), HDM (10 µg/mL *Der f* extract, Citeq), inhibitor treatment (10 µg/mL anti-human TLR4 or dectin-2 neutralizing antibody, both Invivogen, or 10 µg/mL PBP10, Tocris, Bristol, UK), glucocorticoid treatment (1.5 µmol/L dexamethasone, or 1 µmol/L fluticasone propionate, Sigma Aldrich) or siRNA-mediated *APOE* knockdown. Supernatants were harvested for ELISA or liquid-chromatography tandem-mass spectrometry (LC-MS/MS, in 50% methanol [v/v], Applichem) and cells were lysed in RLT buffer with 0.1 % β-mercaptoethanol (Quiagen, Hilden, Germany) or pelleted. All samples were stored at -70°C before analysis.

Normal human bronchial epithelial cells: Commercially available normal human bronchial epithelial cells (NHBE, Lonza, Basel, Switzerland) were expanded for 5-7 days in bronchial epithelial growth medium (BEGM, Lonza) before seeding on 12 mm transwells (Stemcell Technologies, Vancouver, Canada). Upon confluence, apical medium was removed to induce epithelial differentiation and basal medium (PneumaCult-ALI Maintenance Medium, Stemcell Technologies) was exchanged every second day. Trans-epithelial electrical resistance was measured (EVOM2, World Precision Instruments, Sarasota, Florida) to monitor epithelial differentiation. Air-liquid-interface cultured NHBE (ALI-NHBE) were stimulated apically after 6h starvation in PneumaCult-ALI Basal Medium (Stemcell Technologies) with IL-13 (10 ng/mL, Miltenyi) or fluticasone propionate (1.0 µmol/L, Sigma Aldrich). Membranes were cut in half and fixed in formaldehyde (3,5-3,7%) or lysed in RLT buffer (Qiagen). For submerged cultures, NHBE in passage 4 were grown to 90% confluence in BEGM. After overnight starvation in bronchial epithelial basal medium (Lonza), NHBE were stimulated for 24h with purified human ApoE (Merck) or cell-free pooled supernatants from human aMDM at a final concentration of 10% [v/v]. For uptake experiments, NHBE were grown in PneumaCult-Ex Plus medium (Stemcell) on 8-chamber tissue culture-treated glass slides (Falcon polystyrene, Corning), stimulated with 50% MDM supernatant, or blocked with 1 µg/mL human recombinant RAP (Enzo Life Sciences) for 1 h before exposure to 1 µg/mL ApoE (Acrobiosystems, Newark DE, USA). Supernatants and cell lysates were collected and stored as above.

Murine bone marrow derived macrophages

Mice were euthanized using CO_2 and bone marrow cells were flushed from femurs through a 70 µm cell strainer. Bone marrow cells were differentiated at 10^6 cells/mL in complete RPMI1640 20 ng/mL rmM-CSF (Miltenyi) as described above and replated for experiments on day 6-7.

siRNA knockdown

0.25–1.0 × 10^6 macrophages were plated at a density of 1.65 × 10^6/mL in serum-free medium on 24- or 6-well plates. 10 nmol/L siRNA (*APOE* or non-targeting, "scrambled", Horizon Discovery, Waterbeach, UK) was added before 3% [v/v] HiPerfect (Quiagen). After 6h of incubation, medium volume was adjusted to a cell density of 1 × 10^6/mL, and after 24h, all medium was removed and replenished with serum-free RPMI and cytokines for another 24h, during which stimuli were added.

ELISA

ELISA for human ApoE (Mabtech), CCL17, TNF (R&D Systems), IL-6, IL-1β, IL-10 (BD Biosciences), PGE_2 (Cayman Chemical) were used to analyze cell supernatants according to the manufacturer's instructions.

Immunohistochemistry, immunofluorescence staining and confocal microscopy

NHBE seeded on 8-well plastic-chamber slides (IBIDI, Munich, Germany) were fixed in 4% paraformaldehyde (PFA, Sigma-Aldrich). Nasal polyp tissue or turbinates were fixed in PFA, mounted in paraffin and sectioned. Antigen was retrieved by acetone (at -20°C, Merck) for cells or repeated boiling in sodium citrate buffer with 0.05% tween-20 (Merck) for tissues. Slides were blocked using 3% BSA with 10% donkey serum (Thermo Fisher) and stained overnight with primary antibodies for immunofluorescence (ApoE, Atlas Antibodies, Stockholm, SWE; β-actin, Merck; tubulin, Santa Cruz Biotechnology, Dallas, TX, USA; all 1:50, ZO-1, Thermo Fisher, 1:100) before incubation with fluorophore-labeled secondary antibodies (anti-rabbit AF488, anti-goat AF568, anti-mouse-AF658, anti-mouse AF647, all 1:500, Thermo Fisher). Autofluorescence blocking was included for tissues (MaxBlock, ActiveMotif, Waterloo, Belgium). Slides were mounted in DAPI-containing mounting medium (Fluoroshield with DAPI, GeneTex, Irvine, CA, USA, or Fluoromount-G with DAPI, Thermo Fisher) and acquired using a Leica TCS SPF5 II (Leica Microsystems, Wetzlar, Germany) or Zeiss LSM880 Airyscan (Zeiss Microscopy, Jena, Germany) confocal microscope using a 63 × glycerol-immersion objective. Files were adjusted equally for brightness and contrast using ImageJ (U. S. National Institutes of Health, Bethesda, MD, USA). Fluorescence intensity was calculated using MVTec Halcon software. Channels were quantified separately for percentage of area*intensity, adjusted to secondary control. For immunohistochemistry, slides were stained with primary antibodies (p63, Thermo Fisher, MUC5A, Abcam, SCGB1A1, R&D Systems) overnight after pretreatment as noted above. Slides were incubated with a secondary anti-mouse or anti-rat IgG-HRP conjugate and developed using DAB reagent. Images were acquired using a Hamamatsu NanoZoomer S60 microscope.

Ferroptosis analysis

MDM were incubated in the presence of 8.5 µg/mL ApoE and 500 nmol/L RSL3 (Selleckchem, Cologne, Germany) for 2h before supernatant was harvested and analysed by lactate dehydrogenase assay (CyQuant LDH Cytotoxicity Assay, Invitrogen). BMDMs were replated at a concentration of 15.000 cells/well in a 48-well plate on day 6 and stimulated with 10 ng/mL rmIL-4, 10 ng/mL rmIL-13 and 20 ng/mL rmM-CSF (all Miltenyi). After 48h the medium was replaced with fresh complete RPMI1640 with IL-4, IL-13, M-CSF, 1 µmol/L SYTOX Green

Nucleic Acid Stain (ThermoFisher) and treatments. BMDMs were incubated with 500 nmol/L RSL3 and/or 6.8 µg/mL rmApoE (Acrobiosystems) for 25h. Cell death was monitored on a Incucyte SX1 (Sartorius) with the green channel (acquisition time 300 ms).

RNA extraction and qPCR

RNA was extracted from RLT lysates using a spin-column kit according to the manufacturer's instructions (Zymo Research, Freiburg, Germany) and reverse-transcribed using the High Capacity cDNA Reverse Transcription kit (Thermo Fisher). qPCR was performed using FastStart Universal SYBR Green master mix (Roche, Mannheim, Germany) with 10 ng cDNA on a ViiA7 Real-Time PCR System (Applied Biosystems, Thermo Fisher Scientific). Expression levels were normalized to *GAPDH* as house-keeping gene and relative gene expression represented as $2^{-\Delta CT}$ ($\Delta CT = CT_{(housekeeper)} - \Delta CT_{(gene)}$). Primers (4 µmol/L, Metabion Munich, Germany) are listed in Table E1.

QUANTIFICATION AND STATISTICAL ANALYSIS

Transcriptomics

Total RNA quality and quantity was assessed by NanoPhotometer (N60, Implen, Munich, Germany) and with the Agilent 2100 BioAnalyzer (RNA 6000 Nano Kit, Agilent, Santa Clara, CA, USA). For library preparation, strand specific, polyA-enriched 150 bp paired-end RNA sequencing was performed as described earlier (1) on an Illumina HiSeq4000 platform resulting in ~50-118 Million single end reads per library. The STAR aligner (v2.4.2a)(3) with modified parameter settings (--twopassMode=Basic) was used for split-read alignment against the human genome assembly hg19 (GRCh37) and UCSC knownGene annotation. Raw reads were mapped to the human genome (hg38) with GSNAP (version 2018-07-04) (4) and splice-site information from Ensembl release 87 (5). Uniquely mapped reads and gene annotations from Ensembl were used as input for featureCounts (v1.6.2) (6) to create counts per gene, removing all non-protein coding genes. Differential expression was analyzed with R (v3.5.0) and the R package DEBrowser (v1.11.9) (7) using DEseq2 and excluding low coverage features (maximum count >10). Pathway enrichment of DEG was evaluated using the online platform ToppGene suite (https://toppgene.cchmc.org) (8) and volcano plots were created with EnhancedVolcano (v1.1.3) (9). The data is available at www.ebi.ac.uk/arrayexpress; accession number E-MTAB-7962.

Lipid extraction and targeted redox lipidomics

Phospholipids were analyzed as previously described (10). In short, cell pellets were extracted by sequential addition of PBS pH 7.4, methanol (spiked with internal standards 1,2-dimyristoyl-sn-glycero-3-phosphatidylcholine and 1,2-dimyristoyl-sn-glycero-3-phosphatidylethanolamine (DMPC and DMPE, Avanti Polar Lipids, Alabaster AL, USA), chloroform, and saline (final ratio 14:34:35:17). Chromatographic separation using an Acquity UPLC BEH C8 column (130 Å, 1.7 µm, 2.1×100 mm, Waters, Milford, MA) on an ExionLC AD UHPLC system (Sciex, Framingham, MA), was performed as previously described (11) by ramping mobile phase A (water/acetonitrile 90/10, 2 mM ammonium acetate) and mobile phase B (water/acetonitrile 5/95, 2 mM ammonium acetate) from 75 to 85% B over 5 min, to 100% B within 2 min and followed by isocratic elution for 2 min. The LC system was coupled to a QTRAP 6500^{+} mass spectrometer (Sciex), which was equipped with an electrospray source and operated in the negative ion mode. Oxidized 1-stearoyl-2-arachidonoyl-*sn*-glycero-3-phosphatidyl ethanolamine species were analyzed by multiple reaction monitoring based on the

fragmentation of $[M-H]^-$ to arachidonate anions with one to three oxygen incorporated or their secondary fragments using pre-optimized source and compound parameters.

Statistical analysis

All data except transcriptomics was analyzed using GraphPad Prism 9 software (GraphPad Software, La Jolla, Calif). *T* test or Mann-Whitney test were used to compare 2 populations. For comparison of more groups, 2-way ANOVA was used with correction for multiple comparisons. $P < .05$ was considered statistically significant. Details of statistical tests and sample size are provided in the figure legends.

Supplementary References

1. Haimerl P, Bernhardt U, Schindela S, Henkel FDR, Lechner A, Zissler UM, et al. Inflammatory macrophage memory in NSAID-exacerbated respiratory disease. J Allergy Clin Immunol. 2020 Jun;S0091674920308034.
2. Lechner A, Henkel F, Hartung F, Bohnacker S, Alessandrini F, Gubernatorova EO, et al. Macrophages acquire a TNF-dependent inflammatory memory in allergic asthma. J Allergy Clin Immunol. 2021 Dec;S009167492102741X.
3. Dobin A, Davis CA, Schlesinger F, Drenkow J, Zaleski C, Jha S, et al. STAR: ultrafast universal RNA-seq aligner. Bioinforma Oxf Engl. 2013 Jan 1;29(1):15–21.
4. Wu TD, Nacu S. Fast and SNP-tolerant detection of complex variants and splicing in short reads. Bioinformatics. 2010 Apr 1;26(7):873–81.
5. Zerbino DR, Achuthan P, Akanni W, Amode MR, Barrell D, Bhai J, et al. Ensembl 2018. Nucleic Acids Res. 2018 Jan 4;46(D1):D754–61.
6. Liao Y, Smyth GK, Shi W. featureCounts: an efficient general purpose program for assigning sequence reads to genomic features. Bioinforma Oxf Engl. 2014 Apr 1;30(7):923–30.
7. Kucukural A, Yukselen O, Ozata DM, Moore MJ, Garber M. DEBrowser: interactive differential expression analysis and visualization tool for count data. BMC Genomics. 2019 Jan 5;20(1):6.

8. Chen J, Bardes EE, Aronow BJ, Jegga AG. ToppGene Suite for gene list enrichment analysis and candidate gene prioritization. Nucleic Acids Res. 2009 Jul;37(Web Server issue):W305-311.

9. Blighe K, Rana S, Lewis M. EnhancedVolcano: publication-ready volcano plots with enhanced colouring and labeling [Internet]. Available from: https://github.com/kevinblighe/EnhancedVolcano

10. Schwab A, Rao Z, Zhang J, Gollowitzer A, Siebenkäs K, Bindel N, et al. Zeb1 mediates EMT/plasticity-associated ferroptosis sensitivity in cancer cells by regulating lipogenic enzyme expression and phospholipid composition. Nat Cell Biol [Internet]. 2024 Jul 15 [cited 2024 Jul 29]; Available from: https://www.nature.com/articles/s41556-024-01464-1

11. Thürmer M, Gollowitzer A, Pein H, Neukirch K, Gelmez E, Waltl L, et al. PI(18:1/18:1) is a SCD1-derived lipokine that limits stress signaling. Nat Commun. 2022 Dec;13(1):2982.

EXTENDED TABLES AND LEGENDS

Supplementary Table E1: Human primer sequences

	Gene	Forward primer sequence (5' – 3')	Reverse primer sequence (5' – 3')
Housekeeper	***GAPDH***	GAAGGTGAAGGTCGGAGT	GAAGATGGTGATGGGATTTC
Genes	***APOE***	Quiagen QuantiTect Primer Assay Cat.No QT00087297	
	PTGS2	GCTGGAACATGGAATTACCCA	CTTTCTGTACTGCGGGTGGAA
	PTGES	TCAAGATGTACGTGGTGGCC	GAAAGGAGTAGACGAAGCCCAG
	CCL17	AGGGAGCCATTCCCCTTAGA	GCACAGTTACAAAAACGATGGC
	FKBP5	CGGCGACAGGTTCTCTACTTA	GCTGTGGGGCTTTCTTCATTG
	PPBP	TTGGCGAAAGGCAAAGAGGA	GCAATGGGTTCCTTTCCCGA
	IL33	AGCTGGGAAAATCCCAACAGA	AGCAAGATACTCTGTAATAGGTGAA
	SCGB1A1	Qiagen QuantiTect Primer Assay Cat.No. QT00091091	
	CXCL8	GAAGTTTTTGAAGAGGGCTGAGA	TGCTTGAAGTTTCACTGGCAT